

N-TAC (October 29,2002)

Mechanical Structure Analysis and Code Validation

JAERI

Shuichi ISHIKURA

Technical issues in target design

Pressure wave.(Especially, EOS of mercury and FSI*)

*** Fluid-Structure-Interaction.**

Thermal stress.(Presented by Dr. Hino)

Generation of negative pressure in mercury and cavitation.

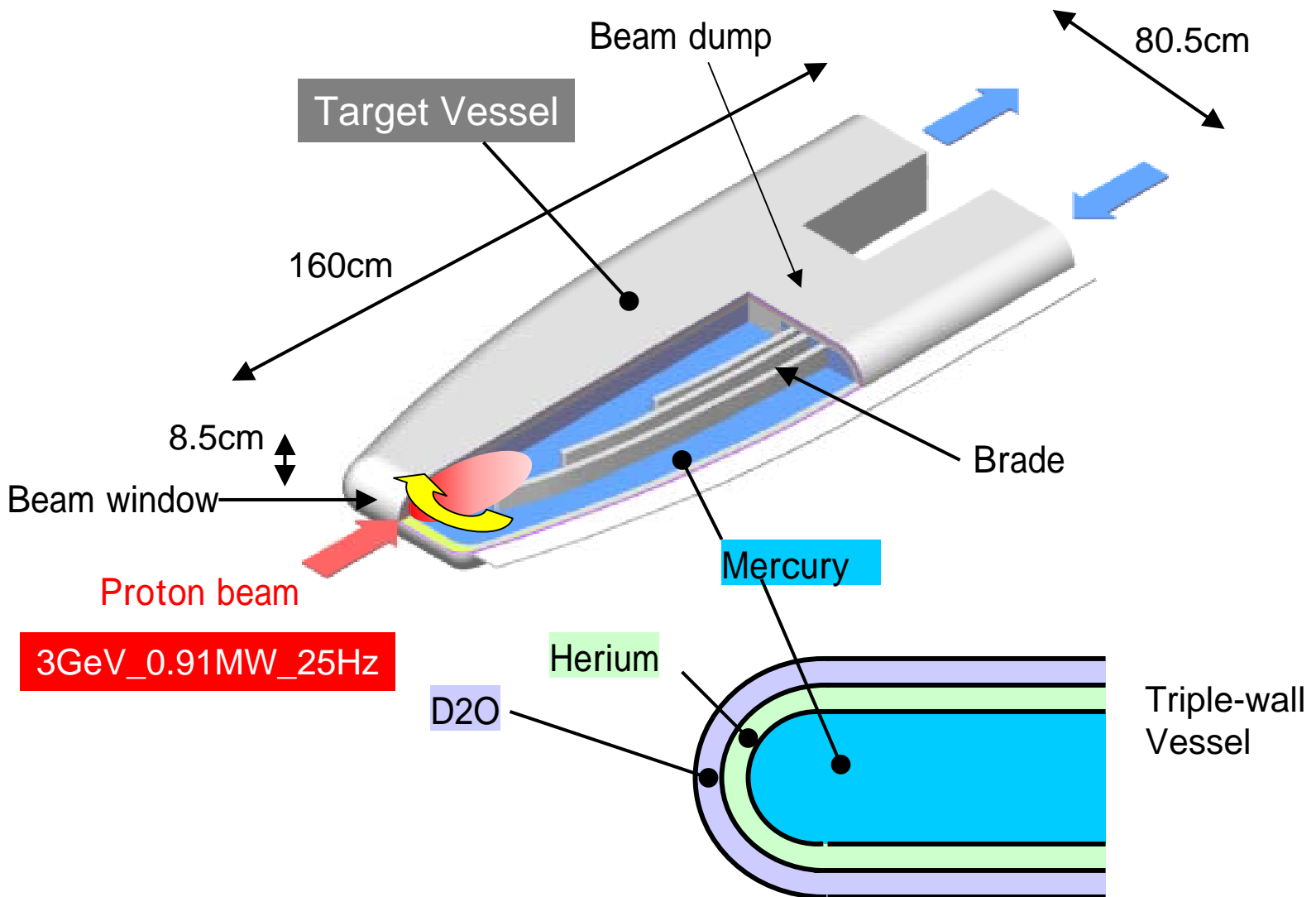
Damage of target container by cavitation erosion.

Material damage because of proton irradiation.

Structural design of target container
under pressure wave

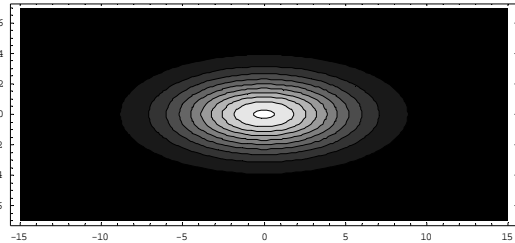
(cavitation is not considered)

Structural concept of liquid mercury target



Distribution of heat deposition in mercury target

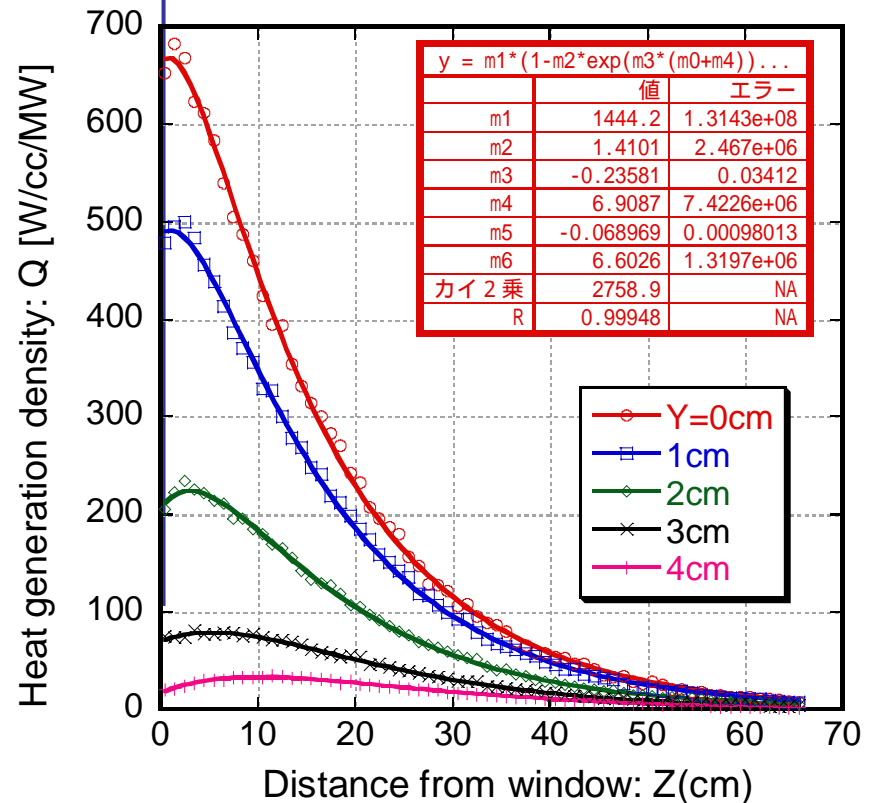
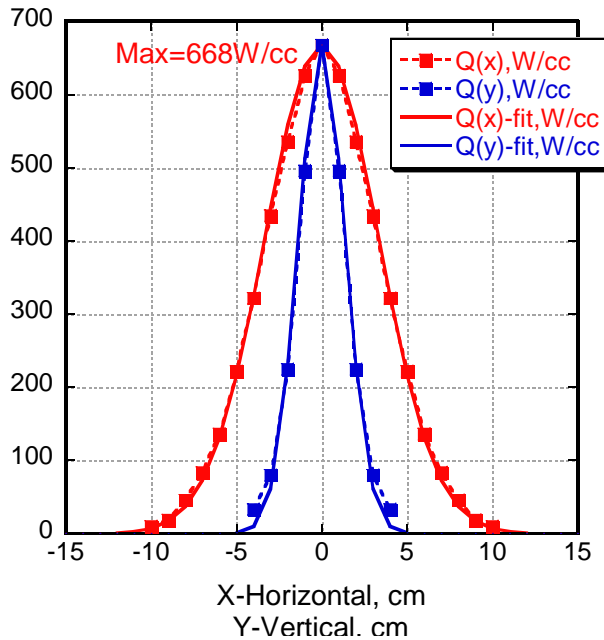
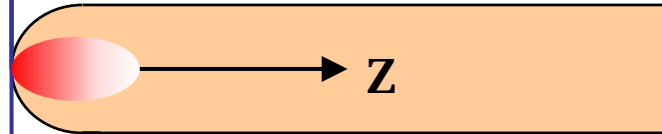
Gaussian distribution



3GeV
0.91MW
25Hz



Analytical code: NMTC/JAM



Temperature rise distribution by heat generation and formation of compression field

Generation of pressure wave in mercury and load on target container. (0.91MW/25Hz)

Injection of pulsed proton beam(1 μ s) :
36.4 kJ/pulse.



Heat generation by nuclear spallation :
 $Q \sim 20$ kJ/pulse.



Max. heat density : $q \sim 26.7$ J/cc/pulse.



Max. temperature rise : $T = q / \rho C_v \sim 17$ /pulse



Max. compressed press. : $P = \alpha T K_s \sim 68$ MPa



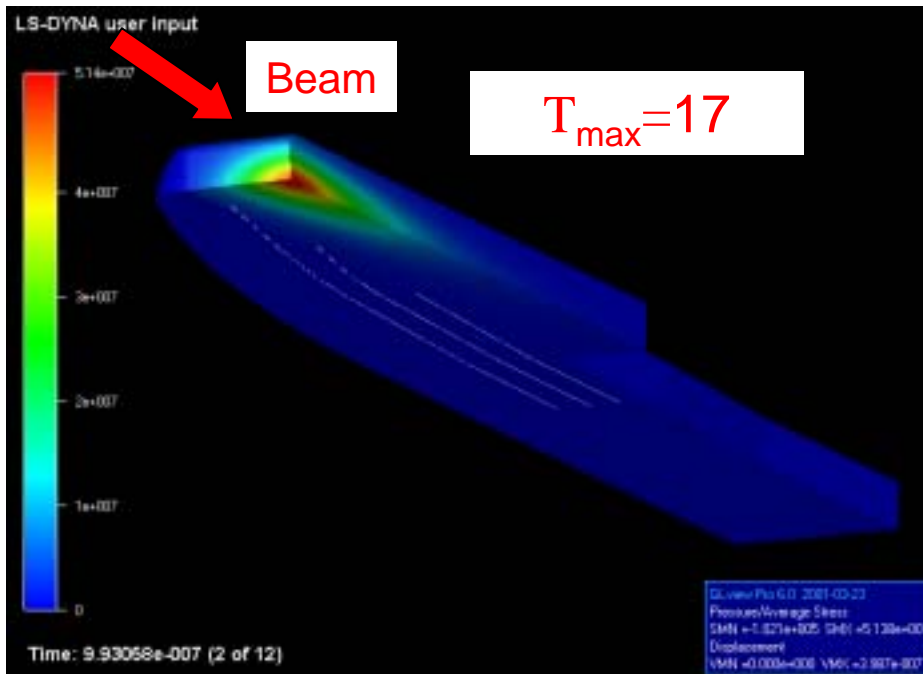
Sound velocity in mercury : $V \sim 1400$ m/s



Load on target container.



Structural integrity of the target container?



Stress evaluation of beam window

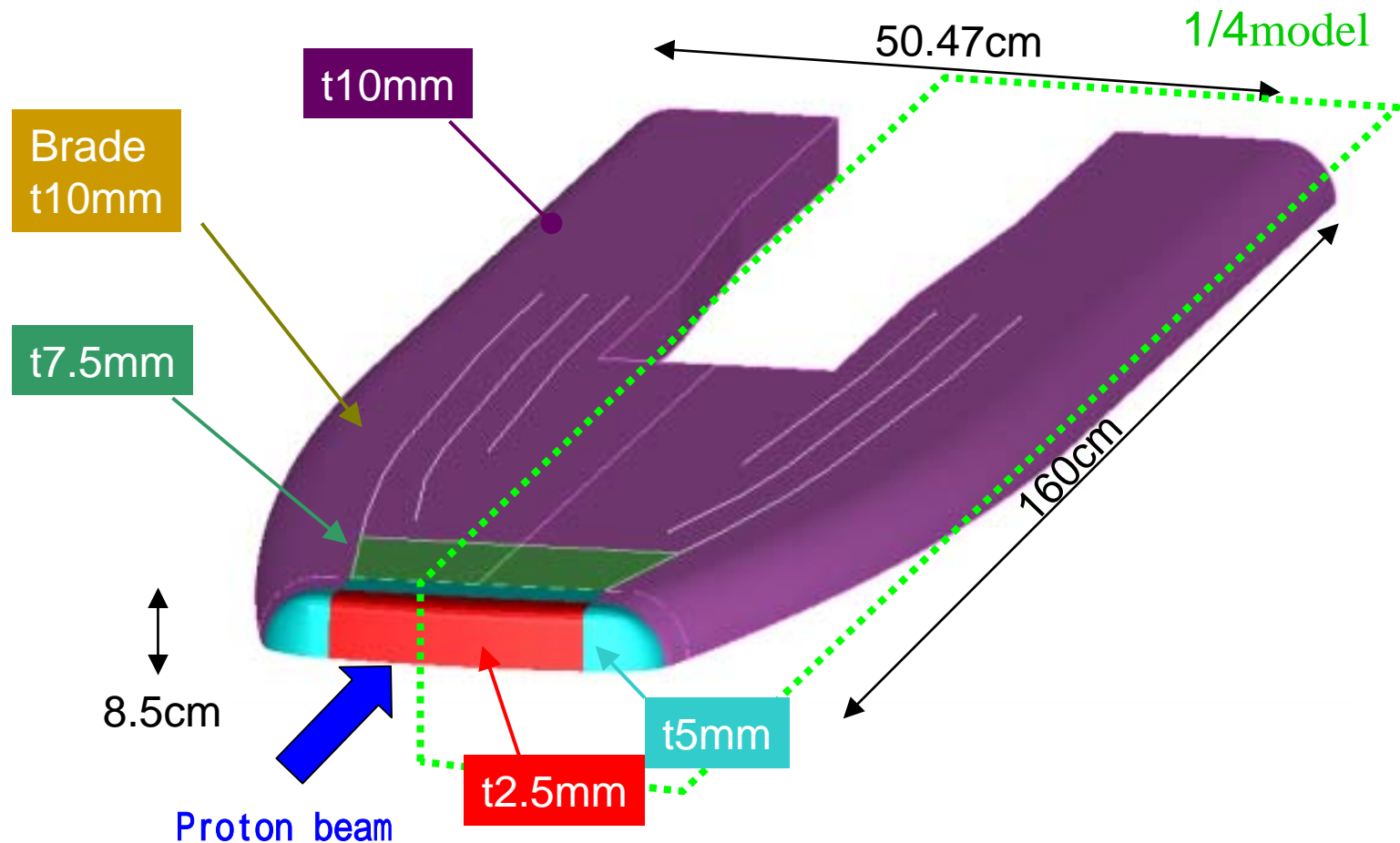
Analytical model (1/4model)

·Code LS-DYNA (Vr .950)

·Number of elements

·Vessel: Shell element 5.16×10^4

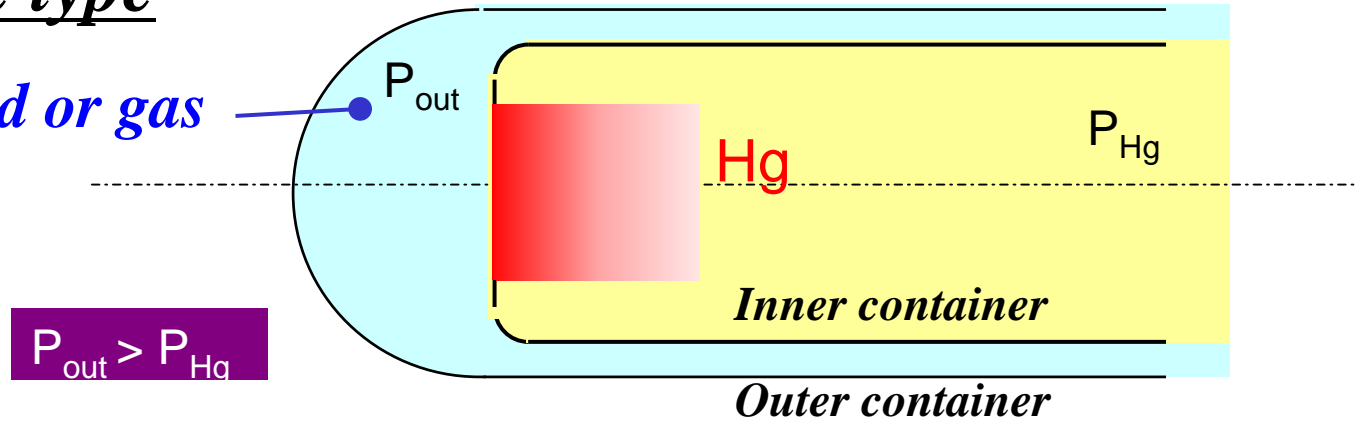
·Hg: Solid element 66.3×10^4



Effect of beam window type on mechanical strength

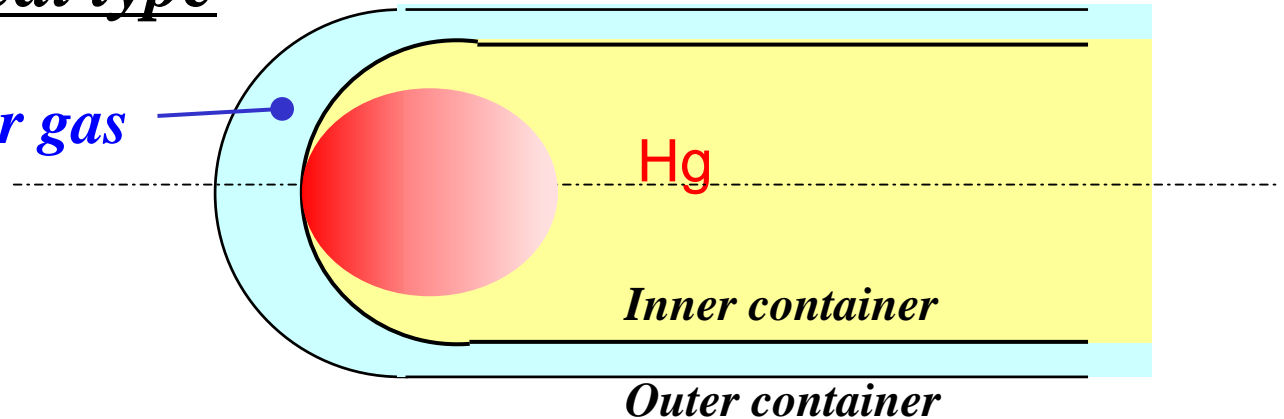
Flat-plate type

Liquid or gas

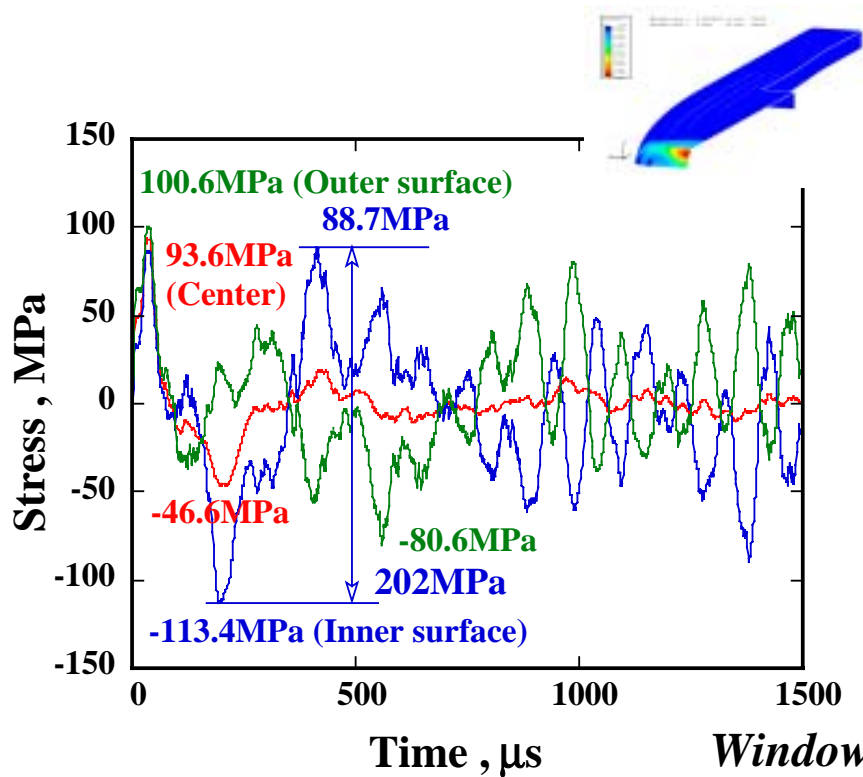


Semi-cylindrical type

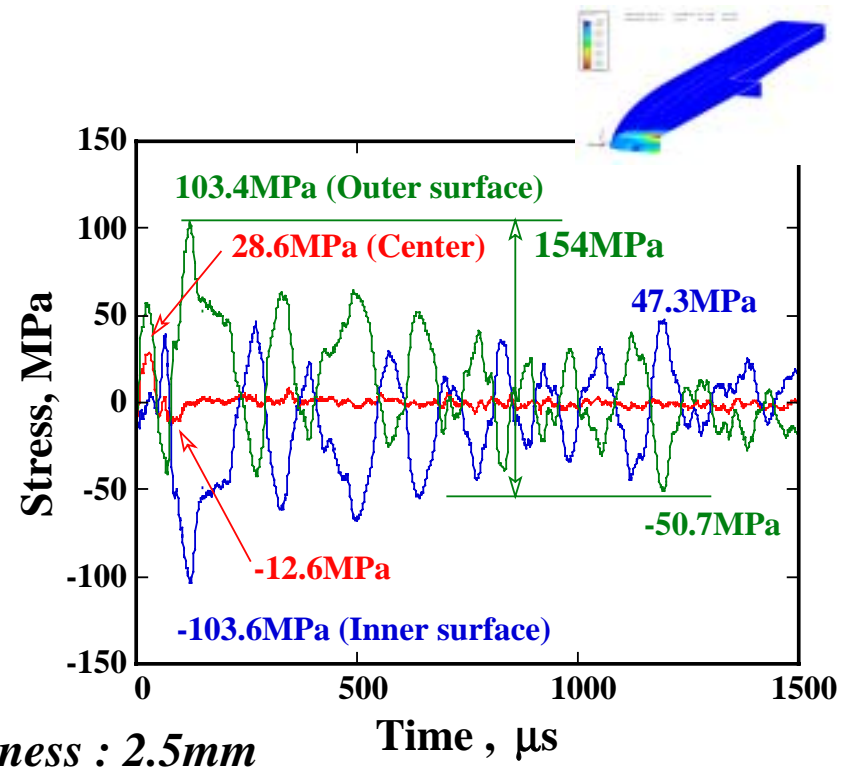
Liquid or gas



Dynamic responses of stress at center of window



Semi-cylindrical type



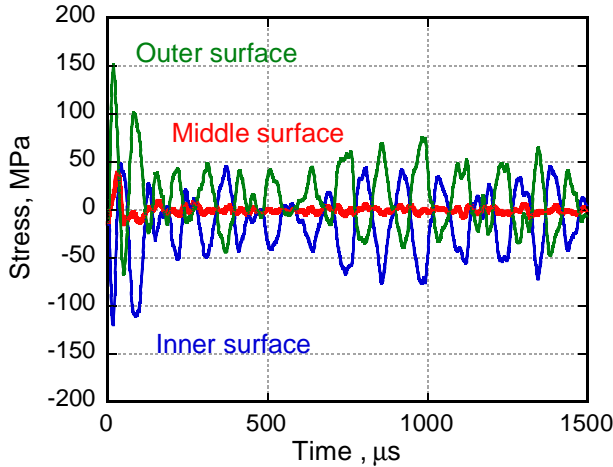
Flat-plate-type

Stress amplitude generated in Flat-plate-type is smaller
→ advantageous for fatigue strength.

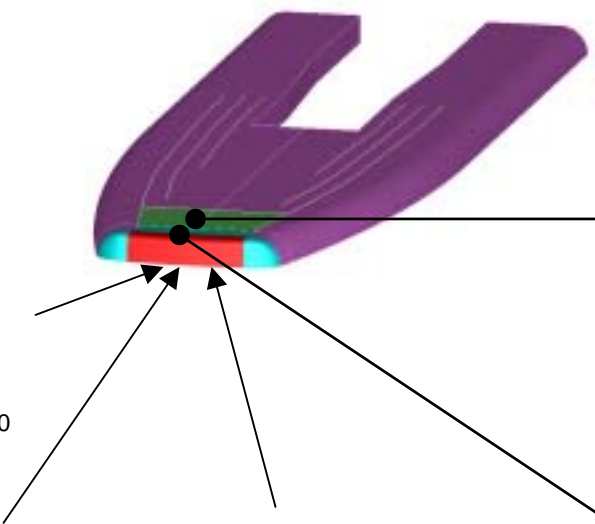
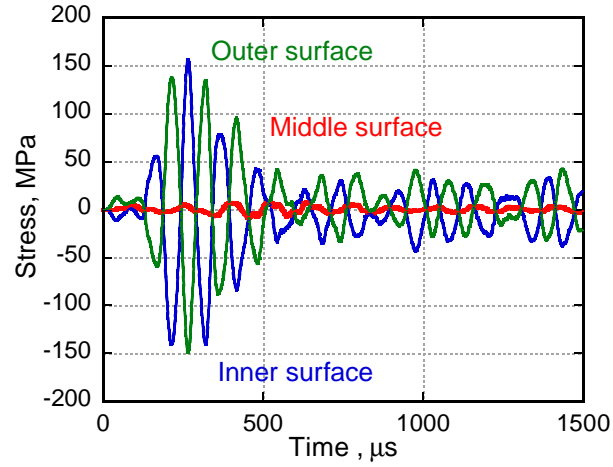
Membrane stress intensity generated in Flat-plate-type is smaller
→ advantageous for instantaneous brake.

Comparison of changes in stress/pressure/displacement at window and upper plate.

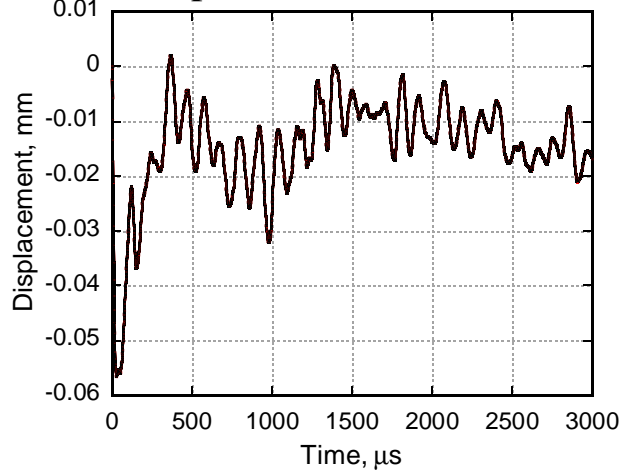
Stresses in center of window



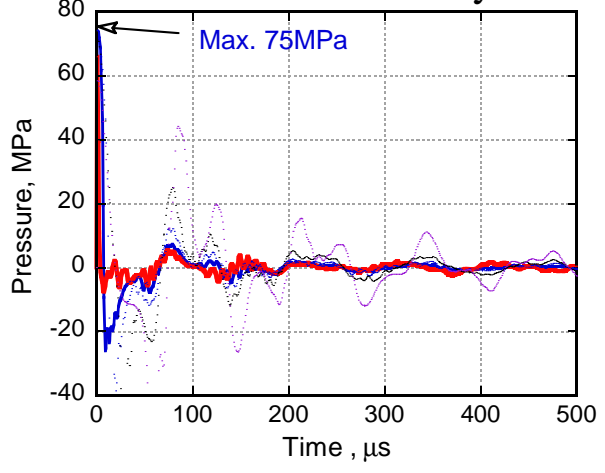
Stresses in upper plate



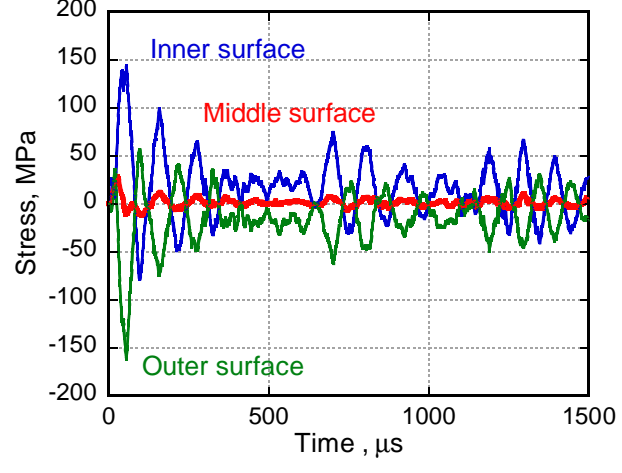
Dip. in center of window



Press. in mercury



Stresses in corner of window

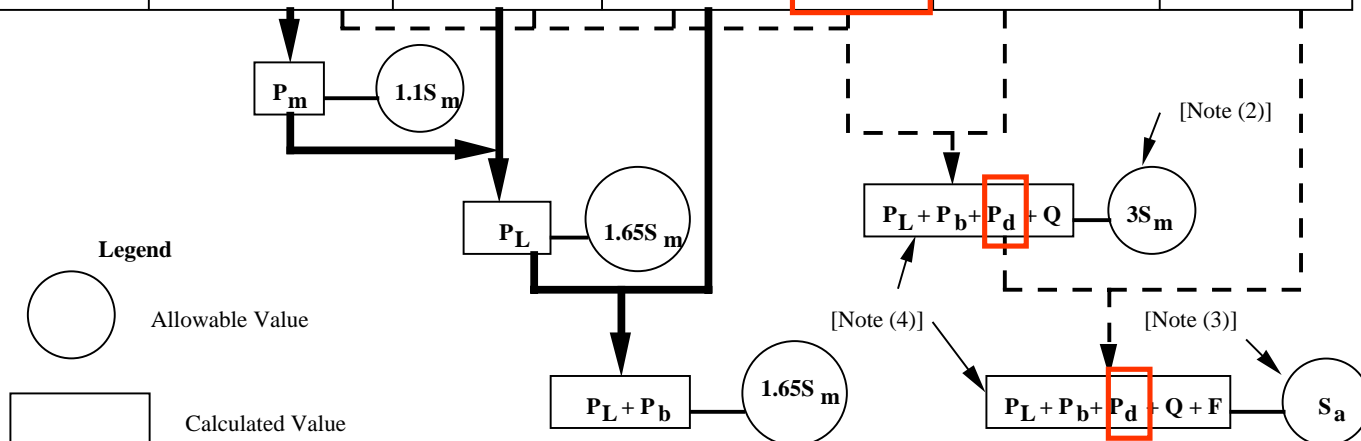


Stress category and allowable stresses

Same as SNS

Normal Service Stress Intensity Limits (SNS)

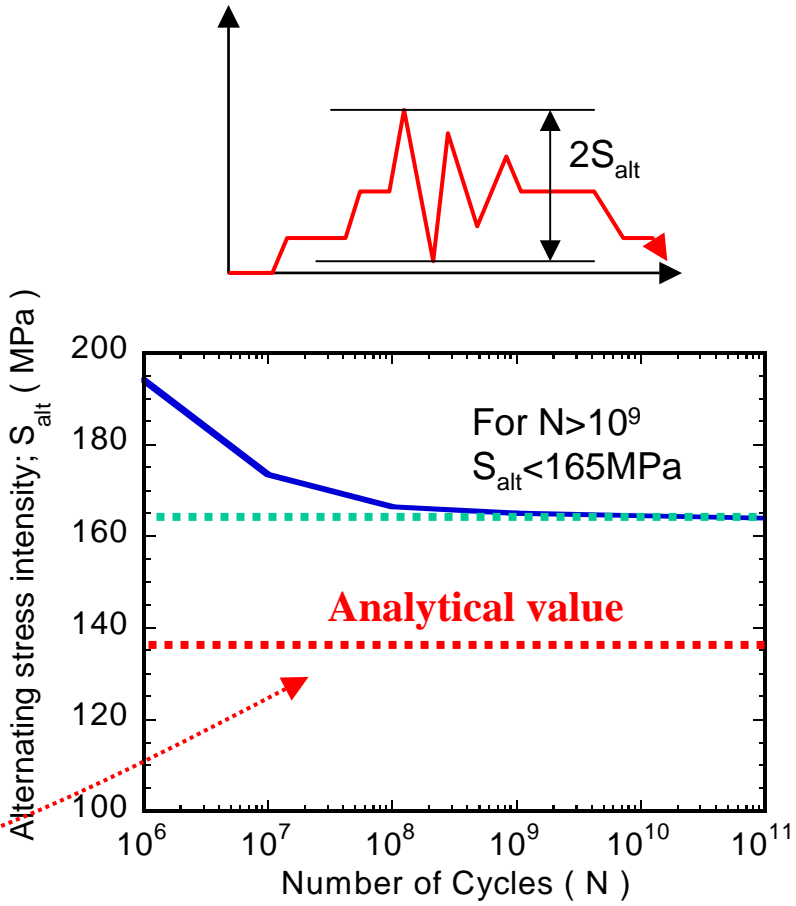
Stress Category [Note (1)]	Primary			Dynamic P_d	Secondary Membrane + Bending Q	Peak F
	General Membrane P_m	Local Membrane P_L	Bending P_b			
Description	Average stress across wall to maintain equilibrium with mechanical loads including pressure and gravity. Excludes discontinuities and stress concentrations.	Average stress across wall from pressure and gravity. Considers discontinuities but not stress concentrations.	Linear bending stress caused by pressure and gravity. Excludes discontinuities and stress concentrations.	Reversing dynamic stress produced by proton pulses	Self-equilibrating stress caused by mechanical loads at structural discontinuities or equivalent linear bending stress due to differential expansion. Excludes local stress concentrations.	(1) Local stress concentration (notch). (2) Non-linear portion of thermal stress. (3) Stress due to shock produced by proton pulses



Maximum stress ranges(2Salt) at main parts of target container by pressure wave

Evaluation part	Max. stress intensity range	Secondary stress range, 3Sm	Fatigue stress range, 2Salt
Center of window	232	345	330
Corner of window	207		
Upper/Under plate	271		

$\times \frac{1}{2} = 136$



Design fatigue curve of SUS316(LN)

Conclusions by pressure wave analyses

- Structural integrity of the flat-plate type beam window of 316(LN)SS is secured against the pressure wave load which generated 1MW proton beam condition.

Analytical evaluation of cavitation erosion

1. Single bubble behavior under pressure change in mercury.
2. Evaluation of shock wave and micro-jet when bubble collapses.
3. Evaluation of the damage of the window wall by Liquid-Solid interaction analyses.

Generation mechanism of cavitation erosion

1. Due to Shock wave

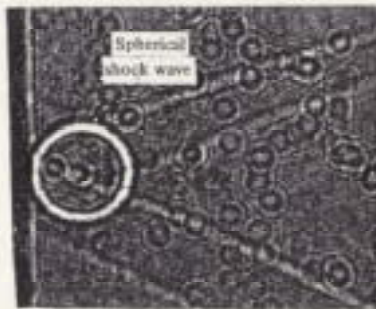
The shock wave generated by rebound following gas bubble shrinkage collides with the solid surface ($P_{\max} \sim \text{GPa}$).

2. Due to micro-jet

Bubble collapses toward the wall, and liquid collide with the solid wall as a micro-jet ($\sim 200\text{m/s}$, $P_{\max} \sim \text{GPa}$)

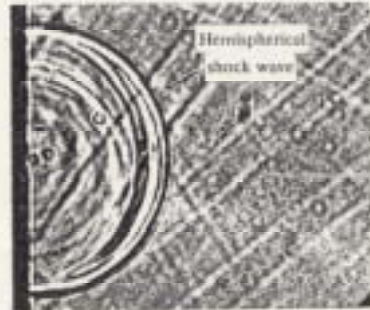
Concept of shock wave generation

Solid wall



(a)

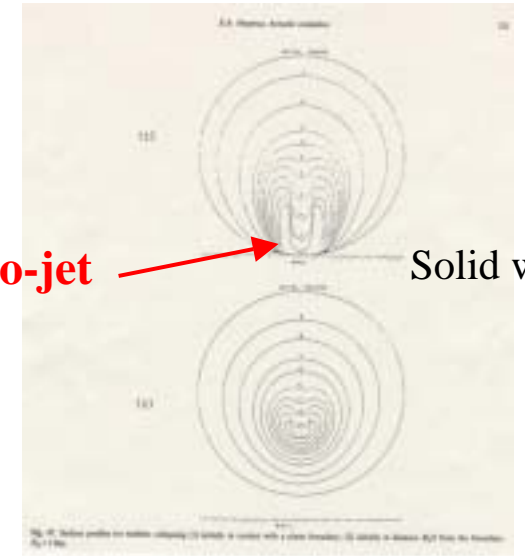
Solid wall



(b)

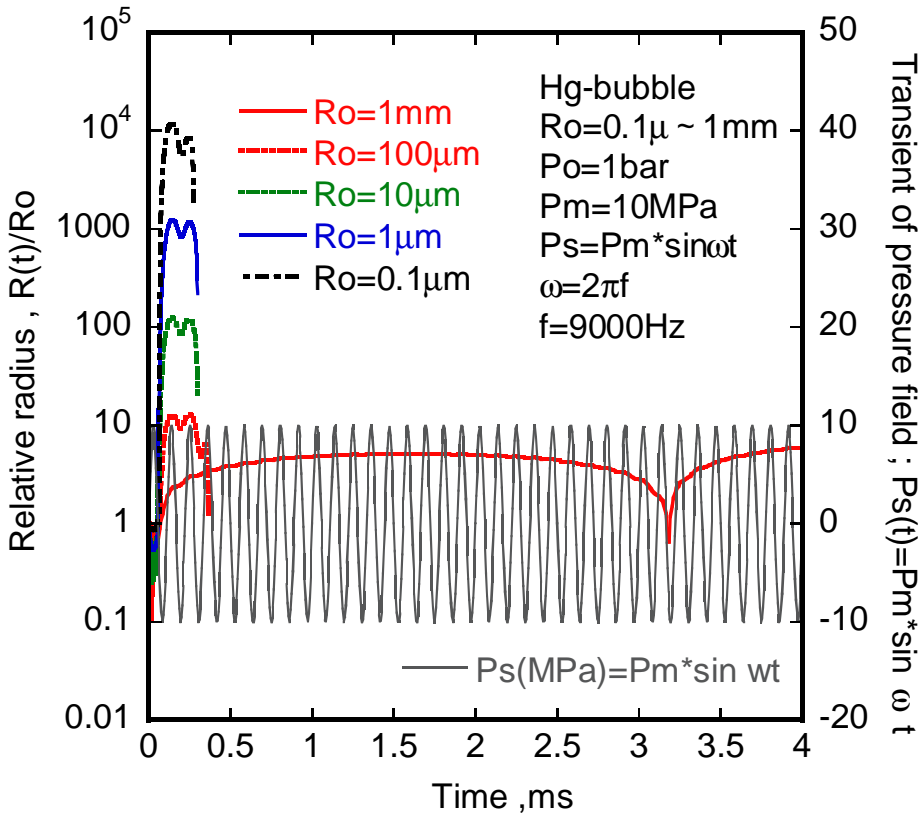
FIGURE 12. The photographs of the shock waves emanating from the bubbles (a) close to, or (b) in contact with, the solid boundary.

Concept of micro-jet generation

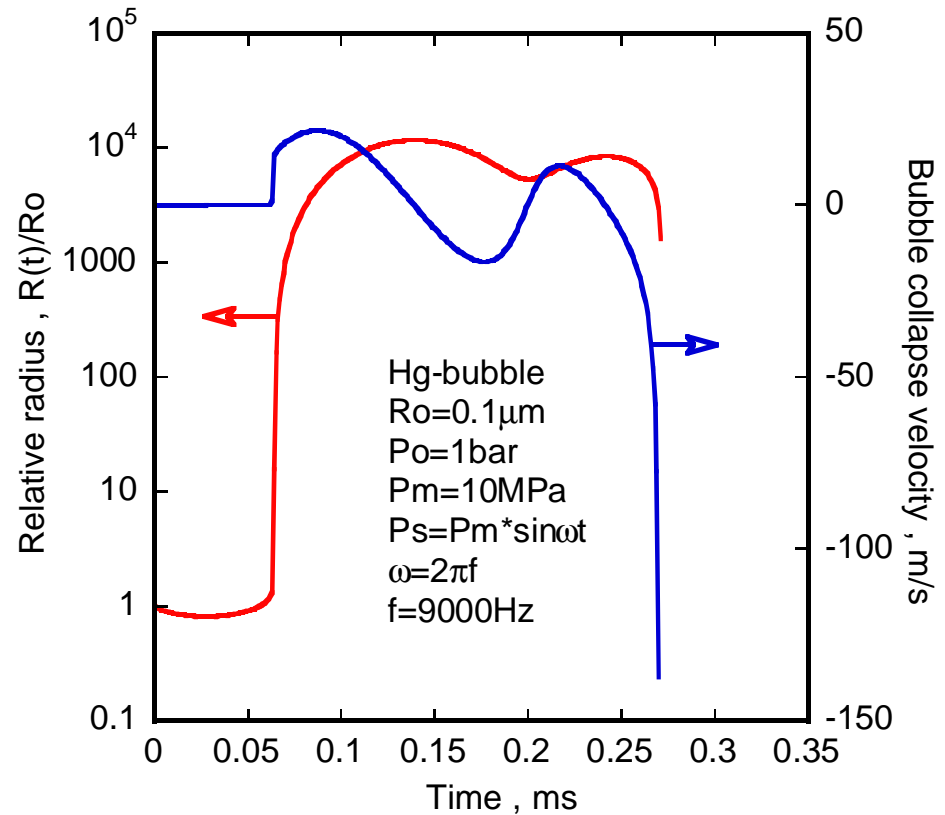


$V=130\text{m/s} \rightarrow 193\text{MPa}(\text{Water})$

Single bubble behavior in mercury



Bubble radius response which is dependent on initial bubble radius. (Bubbles were excited by sine-wave of 10MPa-9kHz.)



Growth and collapse behavior of tiny bubble ($R_0 = 0.1\mu\text{m}$).

The collapse speed of the bubble influences the micro-jet velocity in mercury.

Relationship between collision speed and impact pressure when micro-jet collides with solid wall

Impact power when liquid collides with rigid body wall at speed v ; P_s

$$P_s = \rho_L \times c_L \times v_L$$

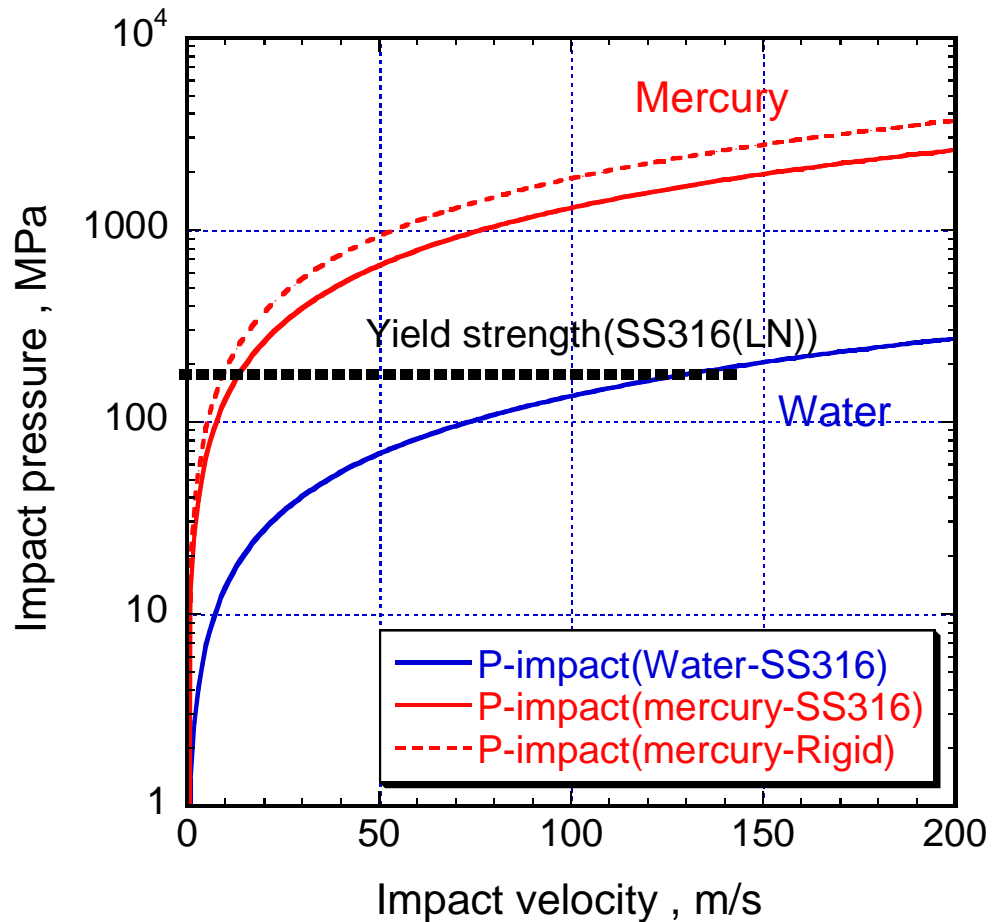
ρ_L : Liquid density

c_L : Sound velocity

v_L : collision velocity

Impact pressure to elastic wall

$$P_{\text{Impact}} = \frac{\rho_{\text{Solid}} c_{\text{Solid}} \rho_{\text{Fluid}} c_{\text{Fluid}}}{\rho_{\text{Solid}} c_{\text{Solid}} + \rho_{\text{Fluid}} c_{\text{Fluid}}} V$$

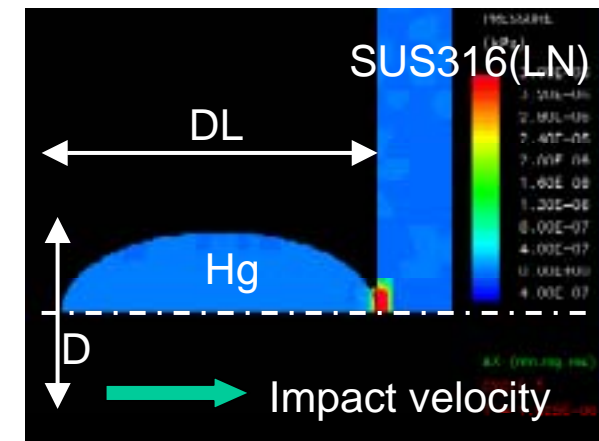
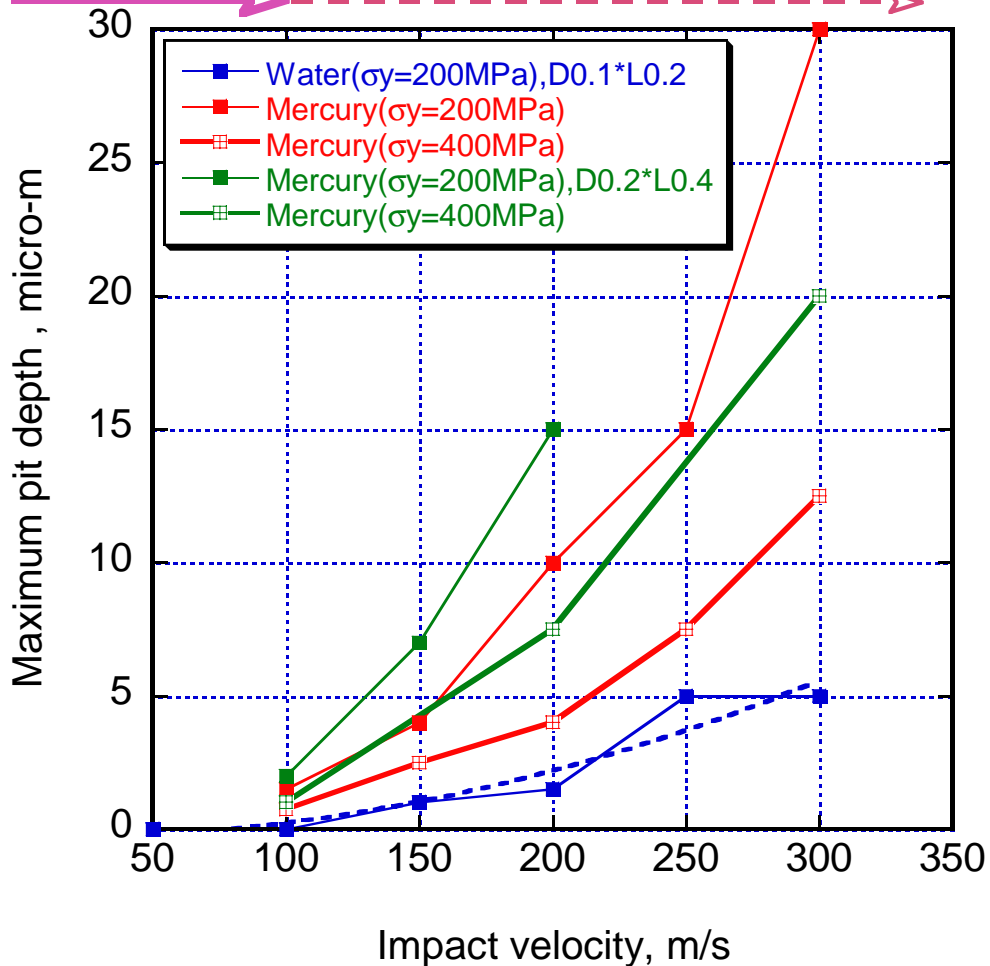


Preliminary analyses of pit formation by collision of mercury micro-jet with solid wall (by AUTODYN)

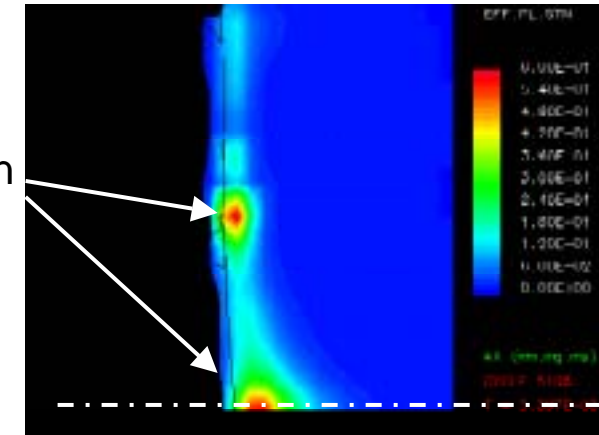
Range of forecast collision speed of water



Range of forecast collision speed of mercury

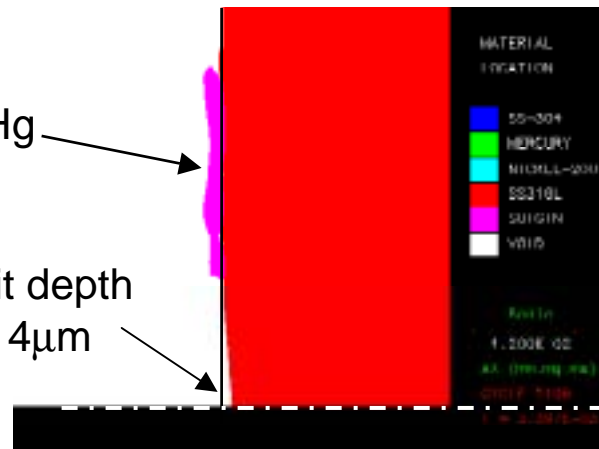


Plastic strain
~ 0.6



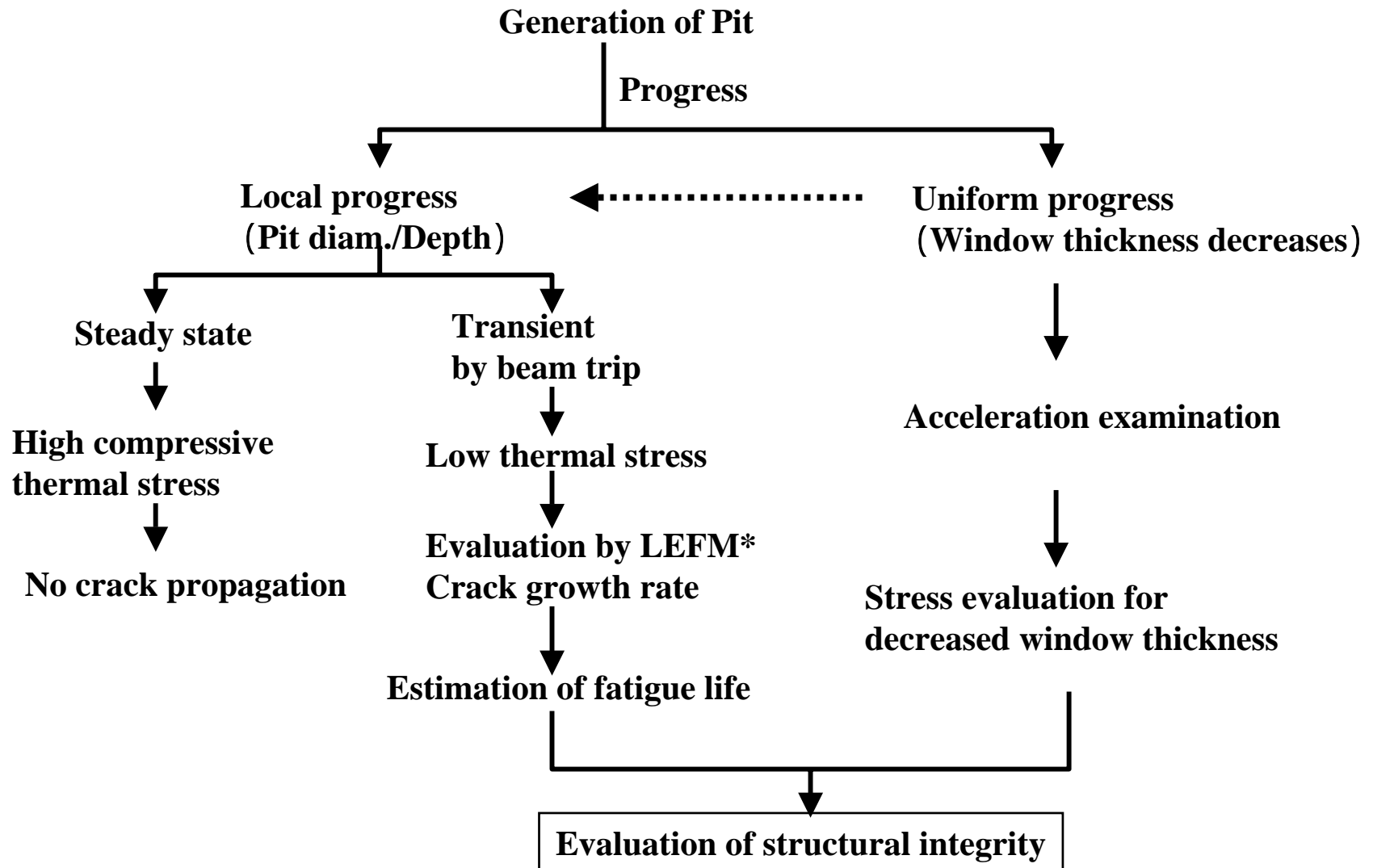
Hg

Pit depth
~ 4 μm



Category to evaluate damage by cavitation erosion.

* LEFM: Linear Elastic Fracture Mechanics



Concept of crack generated around pit

- The bottom of pit is V-notch shape, so it was assumed initial crack. The crack is considered propagating due to alternative pressure wave load. However, structural integrity is secured if the crack does not propagate to the limit crack length.

- High compressive stress field is generated on the inner surface of the flat-plate-type beam window due to the steady state thermal stress.

Therefore, inner surface of the beam window does not become tensile stress field even if the stress by the pressure wave load. The crack generated around pit does not propagate.

- Although the tensile stress would be generated due to beam trip (because the thermal stress decreases), a frequency of this tensile stress generation is too low to affect the cavitation erosion damage.

Future work

1. Experiment work

It is necessary to repeat experiment more than 10^8 cycles under practical operation condition as possible (purity of mercury, stress field, and flow condition).

- to measure the profile of damage, especially depth of pit
- to clarify the damage growth behavior (does it stop or progress?) .

2. Analytical work

It is necessary for pressure wave analyses to consider the EOS of the mercury when the cavitation occurs, because mercury would become the bubbly-liquid state.

→ The bubble-dynamics code is being developed.

It is necessary to analyze the shock wave and the micro-jet behavior near the structure wall which cause erosion

- to clarify the mechanism of cavitation erosion
- to supplement the experimental result.

→ The analyses is being carried out by an existing Euler-Lagrange impact code (preliminary).

Analytical item necessary for target impact analysis and evaluating cavitation damage.

Analytical item	Analytical content	Analytical code	Note and necessary data
Interaction of bubbly-liquid and container	Fluid-Structure interaction analysis which uses nonlinear EOS of Hg which considers dynamic response of bubbly-liquid. The macro behavior of the bubbly-liquid is simulated.	AUTODYN DYTRAN RADIOSS Etc.	· Nonlinear EOS of bubbly-Hg. · Direct coupling of bubbly-liquid equations.
When bubble collapses · Formation of micro jet	Formation of micro jet when bubble collapses in mercury. (Stagnant and flowing condition)	FLUENT FROW-3D Etc.	· Is it possible because of the potential flow?
	Elasto-Plastic interaction with solid wall by micro jet when bubble collapses in mercury.	AUTODYN DYTRAN RADIOSS	· Nonlinear EOS of bubbly-Hg. · Strain rate hardening. $d\epsilon/dt = \sim 10^7$
When bubble collapses · Formation of shock wave.	Elasto-Plastic interaction with solid wall by shock wave when bubble collapses in mercury.	Ditto	Ditto
Evaluation of pit progress.	The pit progress is evaluated by the condition of the design analysis result (negative pressure) based on the experimental data.	There is a necessity for developing the code.	· Process of pit progress · Pit profile.
Evaluation of fatigue life.	Fatigue damage evaluation by which irradiation hardening to load cycles in target operation life. Fracture mechanics evaluation by which “Pit+Crack” is assumed.	There is a necessity for developing the code.	Irradiation effect at crack growth rate

END